Reducing Low-Rank Interference to Improve Environmental Estimation from Ambient Sound

John Lipor
Dept. of Electrical & Computer Engineering
Portland State University
Email: lipor@pdx.edu

John Gebbie
Metron, Inc.
Email: gebbie@metsci.com

Martin Siderius
Dept. of Electrical & Computer Engineering
Portland State University
Email: siderius@pdx.edu

***Abstract*—Hypothesis testing presents an efficient means of partitioning the seabed into regions of similar geoacoustic properties. Ambient sound collected by an autonomous vehicle towing a vertical line array (VLA) can be used to characterize the seabed over large regions of interest. However, additional sound sources such as passing ships result in low-rank interference that can make accurate hypothesis testing impossible. We present a non-convex optimization procedure for removing low-rank interference from covariance matrices formed from a VLA. We describe an alternating optimization algorithm and an intelligent initialization procedure that allows us to efficiently recover the uncorrupted covariance matrix. On synthetic data, we show that our approach can allow for reliable hypothesis testing even in the presence of very strong interference. We also demonstrate that recordings from the New England Shelf Break Acoustics experiment contain low-rank interference that disrupts hypothesis testing, and that our method can adequately mitigate this interference, restoring the area under the receiver operating characteristic curve to 1.0.**

***Index Terms*—ambient noise, covariance estimation, low-rank approximation, hypothesis testing, geoacoustic inversion**

I. Introduction

The geoacoustic parameters of the ocean floor are known to impact the propagation of sound, playing a critical role in sonar performance prediction [1]. To enable seabed characterization over large spatial regions, researchers have developed methods for geoacoustic inversion from passive sources such as crashing waves [2]. Since these methods do not rely on active sources, they can utilize data recorded from drifting buoys or autonomous vehicles [3], [4], making them amenable to characterization over large spatial regions. However, results on real-world data indicate that methods such as that proposed in [2] lack robustness due to model mismatch. Among the leading causes of such mismatch are disturbances to the ambient noise field, especially those due to passing ships.

We consider the problem of partitioning the seabed according to the types defined by the High Frequency Environmental Acoustics (HFEVA) dataset [5]. When the ambient sound is dominated by crashing waves, this may be framed as a hypothesis testing problem, which was studied extensively in [6]. However, low-rank interference from sources such as passing ships can cause large deviations from the underlying model, degrading the performance of hypothesis testing and geoacoustic inversion. Historically, such deviations are handled through robust hypothesis testing methods, which aim to allow for accurate testing in the presence of model mismatch [7]. These methods tend to emphasize deviation from a nominal distribution (e.g., Gaussian), with the goal of providing strong performance without normal assumptions [8], [9] or in high-dimensional settings [10], [11]. While these methods may have applicability to our setting, they do not provide a way to mitigate interfering signals such as those considered here.

In this work, we present an approach to mitigating low-rank interference for vertical line arrays (VLAs) with uniform inter-element spacing. We leverage the fact that, for such arrays, the ideal covariance matrix has Toeplitz structure [12], enabling us formulate interference mitigation as a non-convex optimization problem that can be solved by alternating methods. We provide an intelligent initialization for this problem that allows us to dramatically improve hypothesis testing performance, even in the presence of very strong interferers. We demonstrate the efficacy of our approach on both simulated ambient sound and experimental data from the New England Shelf Break Acoustics (NESBA) experiment [3], [13].

II. Problem Formulation

Consider a VLA with M elements and uniform inter-element spacing. In the ideal setting, the ambient sound is generated by crashing waves at the surface and has well-understood statistical properties that can be leveraged for geoacoustic inversion [2]. Let the N-dimensional vector of geoacoustic parameters of interest be $\theta \in \mathbb{R}^N$. In this case, the Fourier-transformed snapshots at a single frequency are vectors $x \in \mathbb{C}^M$ and are assumed to be circularly-symmetric Gaussian with zero mean and covariance

$$K_\theta = \mathbb{E}[xx^H] = \sigma_s^2 \Gamma_\theta + \sigma_n^2 I, \tag{1}$$

where σ_s^2 is the power in the ambient noise, σ_n^2 is the non-acoustic sensor noise variance, and Γ_θ is the signal covariance matrix obtained from a model of the ambient sound [12]. This signal covariance matrix is normalized so that $\mathrm{tr}\,(\Gamma_\theta) = M$.

Motivated by interfering sound, such as that generated by a passing ship, we wish to mitigate strong low-rank interference. In this setting, we model the received snapshots as $y = x + z$,

J. Lipor was supported by Defense Advanced Research Projects Agency YFA award 454 D22AP00135 and National Science Foundation award CAREER CIF-2046175. M. Siderius 455 was supported by Office of Naval Research Ocean Acoustics Program Grant numbers 456 N00014-19-1-2720 and N00014-23-1-2070.

where $z \in \mathbb{C}^M$ has covariance $\mathbb{E}[zz^H] = \sigma_i^2 QQ^H$ for some $Q \in \mathbb{C}^{M\times r}$ normalized so that $\text{tr}\left(QQ^H\right) = M$, yielding an interference strength σ_i^2. Assuming x and z are uncorrelated, the interfering ship results in the covariance

$$\bar{K}_\theta = \sigma_s^2\Gamma_\theta + \sigma_n^2 I + \sigma_i^2 QQ^H = K_\theta + \sigma_i^2 QQ^H. \quad (2)$$

As stated in the introduction, we consider the problem of hypothesis testing for changes in the geoacoustic parameters of the seabed, where we wish to test whether these parameters are equal at two locations w_0 and w_1. Under the zero-mean complex normal assumption above, this becomes a test for equality of covariance, for which Box's M Test is the classical solution [14]. Suppose two collections of snapshots $\left\{y_1^{(0)}, \ldots, y_L^{(0)}\right\}$ and $\left\{y_1^{(1)}, \ldots, y_L^{(1)}\right\}$ are obtained at locations w_0 and w_1, respectively, yielding sample covariance matrices $\hat{K}_0$ and $\hat{K}_1$. Box's M Test yields the test statistic

$$\begin{aligned}\Lambda \quad = \quad & 2L\log\det\left(\hat{K}_{\text{pool}}\right) - L\log\det\left(\hat{K}_0\right) \\ & -L\log\det\left(\hat{K}_1\right), \end{aligned} \quad (3)$$

where $\hat{K}_{\text{pool}} = \frac{1}{2}\left(\hat{K}_0 + \hat{K}_1\right)$ is the pooled covariance matrix. Hypothesis testing proceeds by comparing (3) to some fixed threshold, chosen either by bootstrapping or by the asymptotic distribution of the test statistic, which is known to be χ^2 [15]. While hypothesis testing has been applied successfully to differentiate between distinct seabed types [6], strong interference can cause the performance of hypothesis testing to deteriorate rapidly. This is especially pertinent when performing sensing from ambient sound, where the signal-to-noise ratio (SNR) is much lower than when actively transmitting. Therefore, methods for mitigating such interference are essential for facilitating large-scale exploration of the geoacoustic properties of the seabed.

III. Interference Mitigation Approach

We now present an optimization procedure for mitigating low-rank interference of the form laid out above. Let $\hat{K}$ be the observed sample covariance from some location containing both a signal and interference portion, as well as additive noise. To recover the uncorrupted covariance only, we wish to remove the rank-r interference defined by Q, solving

$$\begin{aligned} \min_{\substack{K\in\mathbb{C}^{M\times M}\\ Q\in\mathbb{C}^{M\times r}}} \quad & \left\|\hat{K} - K - QQ^H\right\|_F^2 \\ \text{subject to} \quad & K \in \mathcal{S}\cap\mathcal{T}, \end{aligned}$$

where $\mathcal{S}$ and $\mathcal{T}$ are the sets of positive semidefinite (PSD) and Toeplitz matrices, respectively. The above problem is non-convex, since it contains a fourth-order term in Q. However, by using variable splitting we arrive at the following bi-convex problem

$$\begin{aligned} \min_{\substack{K\in\mathbb{C}^{M\times M}\\ Q,W\in\mathbb{C}^{M\times r}}} \quad & \left\|\hat{K} - K - QW^H\right\|_F^2 \quad (4) \\ \text{subject to} \quad & K \in \mathcal{S}\cap\mathcal{T} \quad (5) \\ & Q = W, \end{aligned}$$

Algorithm 1 Initialization procedure for covariance and interference estimation.

Input: observed sample covariance $\hat{K}$, interference rank r, slope parameter ℓ

Output: initial estimates $K_{(0)}$, $Q_{(0)}$, $W_{(0)}$

obtain eigenvalue decomposition $\hat{K} = \sum_{i=1}^M \lambda_i u_i u_i^H$
$\bar{\lambda}_i \leftarrow \lambda_i,\ i = r+1, \ldots, M$
$s \leftarrow$ estimated slope of eigenvalues $\lambda_{r+1}, \ldots, \lambda_{r+\ell}$
for $i = r, \ldots, 1$ **do**
  $\bar{\lambda}_i \leftarrow \lambda_{r+1} + (r-i+1)s$
  $\gamma_i \leftarrow \sqrt{\max\left\{1\times 10^{-6}, \lambda_i - \bar{\lambda}_i\right\}}$
end for
$K_{(0)} \leftarrow \sum_{i=1}^M \bar{\lambda}_i u_i u_i^H$
$Q_{(0)} \leftarrow \sum_{i=1}^r \gamma_i u_i$
$W_{(0)} \leftarrow \sum_{i=1}^r \gamma_i u_i$

which is convex in Q for a fixed K and W, and likewise is convex in W for a fixed K and Q. Although still non-convex, this formulation facilitates the application of alternating minimization procedures such as alternating direction method of multipliers (ADMM) [16]. Consider the augmented Lagrangian

$$\begin{aligned} J(K,Q,W,\beta) = & \left\|\hat{K} - K - QW^H\right\|_F^2 + \beta^H(Q-W) \\ & + \frac{\rho}{2}\left\|Q-W\right\|_F^2, \end{aligned} \quad (6)$$

where $\rho > 0$ is a tuning parameter and $\beta \in \mathbb{C}^{M\times r}$ is the matrix of Lagrange multipliers. Optimization of (6) proceeds in an alternating fashion, sequentially minimizing over each variable while keeping the others fixed. In the case of K, the PSD and Toeplitz constraint is satisfied by projecting the result onto the set $\mathcal{S}\cap\mathcal{T}$ via Dykstra's method [17]. For both Q and W, the problem admits a closed form solution. Beginning with initial guesses for $K_{(0)}, Q_{(0)}, W_{(0)}$ described below and $\beta_{(0)} = 0_{M\times r}$, this approach follows the iterations

$$\begin{aligned} K_{(k+1)} &= P_{\mathcal{S}\cap\mathcal{T}}\left(\hat{K} - Q_{(k)}W_{(k)}^H\right) \\ Q_{(k+1)} &= \left[2\left(\hat{K} - K_{(k+1)}\right)W_{(k)} - \beta_{(k)} + \rho W_{(k)}\right] \\ &\quad \left(2W_{(k)}^H W_{(k)} + \rho I\right)^{-1} \\ W_{(k+1)} &= \left[2\left(\hat{K} - K_{(k+1)}\right)Q_{(k+1)} + \beta_{(k)} + \rho Q_{(k+1)}\right] \\ &\quad \left(2Q_{(k+1)}^H Q_{(k+1)} + \rho I\right)^{-1} \\ \beta_{(k+1)} &= \beta_{(k)} + \rho\left(Q_{(k+1)} - W_{(k+1)}\right), \end{aligned}$$

where $P_{\mathcal{S}\cap\mathcal{T}}(A)$ denotes the projection of the matrix A onto the intersection of PSD, Toeplitz matrices.

For non-convex problems such as (4), the choice of initialization has a major impact on the resulting solution, and initialization close enough to the global optimum can often result in global convergence results [18], [19]. Further, we note that there is an identifiability issue with the problem

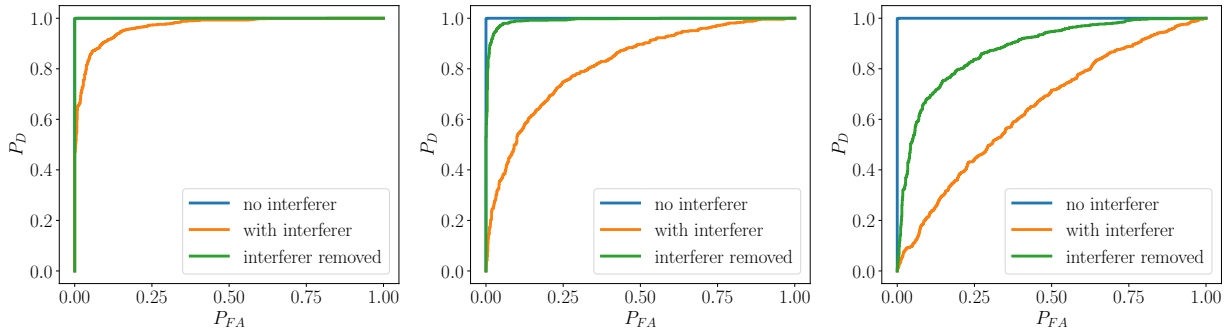

(a) (b) (c)

Fig. 1. ROC curves when testing HFEVA Type 5 vs. Type 8 in the presence of interference of varying rank. (a) Interference rank $r = 2$, (b) $r = 4$, (c) $r = 8$. The proposed recovery method achieves an AUC above 0.9 for both (a) and (b).

(4), since a portion of the matrix QW^H may lie in the set $\mathcal{S} \cap \mathcal{T}$. Fortunately, as long as the interference covariance is sufficiently low-rank relative to the signal covariance K_θ, an accurate estimate can be obtained. To obtain such an estimate, note that a strong rank-r interferer following the model (2) will result in r eigenvalues that are larger than all others, making the interference subspace is easy to identify. However, removing this subspace entirely may destroy the ability to perform hypothesis testing if the interferer is correlated with the principal eigenvectors of either signal covariance matrix. To estimate the strength of the interference, we utilize the fact that for a Wishart matrix, the eigenvalues follow a Marchenko-Pastur distribution in the limit and are therefore smoothly increasing. We estimate this increase as a linear function whose slope is taken as the average slope of eigenvalues $r + 1$ to $r + \ell$ for some $\ell > 0$. Our initial $K_{(0)}$ is then formed by reducing the first r eigenvalues to maintain a linear slope, with $Q_{(0)} = W_{(0)}$ formed by taking the rank-r estimate of the residual. In practice, we set $\ell = 10$ and do not find the result to depend heavily on this choice. Pseudocode for this procedure is given in Alg. 1. In practice, we set $\ell = 10$ and do not find the result to depend heavily on this choice.

IV. Empirical Results

We evaluate our recovery method on both synthetic data and recordings from the NESBA experiment [3]. For synthetic data, we generate snapshots using the multidimensional ambient noise model (MDANM) [20], which is an implementation of the Harrison model [12], assuming a 32-element VLA with 0.15 m element spacing and a frequency of 4.5 kHz. We assume a SNR of 10, setting $\sigma_s^2 = 10$ and $\sigma_n^2 = 1$ in (1). To generate synthetic interference, we follow the approach of [21] and optimize the interference covariance to make hypothesis testing as difficult as possible (i.e., to minimize the likelihood ratio test statistic). When applying our recovery algorithm, we set the parameter $\rho = 1 \times 10^4$ and iterate until $\|K_k - K_{k+1}\|_F < 1 \times 10^{-6}$.

We show the receiver operating characteristic (ROC) curves for testing HFEVA sediment Type 5 (Very Coarse Gravel) vs. Type 8 (Gravelly Muddy Sand) in Fig. 1, where "interferer removed" denotes the ROC curve after applying our recovery method. In the rank-2 case, the area under the curve (AUC) is reduced to 0.96 by the interference and returned to 1.0 by applying our approach. For a rank-4 interferer, the AUC is reduced to 0.82 and returned to 0.99 by our method. Finally, for a rank-8 interferer, the AUC is reduced to 0.65 and returned to 0.88, indicating that our proposed recovery method can make hypothesis testing feasible to some degree even for very significant corruptions.

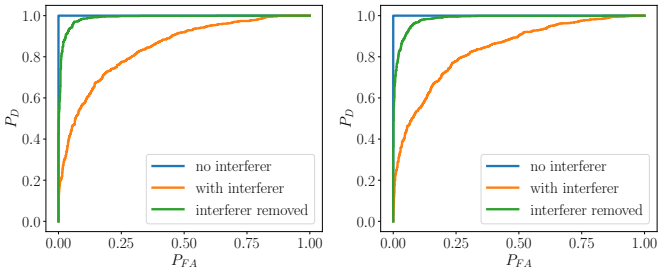

(a) (b)

Fig. 2. ROC curves under a rank-10 interferer when testing (a) Type 11 vs. Type 6 and (b) Type 11 vs. Type 14. In both cases, the proposed recovery method returns the AUC to above 0.98.

Fig. 2 shows the ROC curves for testing HFEVA Type 11 (Fine Sand) against (a) Type 6 (Muddy Sandy Gravel) and (b) Type 14 (Clayey Sand). Since these seabed types are more easily distinguished, we consider a rank-10 interferer. In both cases, the interference reduces the AUC to 0.84. Likewise, our recovery method returns the AUC to 0.99 for Type 11 vs. Type 6 and to 0.98 for Type 11 vs Type 14. Although not pictured, we tested our recovery approach across a wide variety of seabed types and found similar results, with the degree of recovery depending on the interference rank as in Fig. 1.

Finally, we consider the applicability of our recovery method in the context of parameter estimation through vertical directionality and bottom loss curves. We show the corrupted and recovered vertical directionality curves in the presence of a rank-2 interferer for a variety of types in Fig. 3. Since estimation is a more difficult task than hypothesis testing, we set the SNR to 20 dB and set the interference strength 10 dB above the signal level.

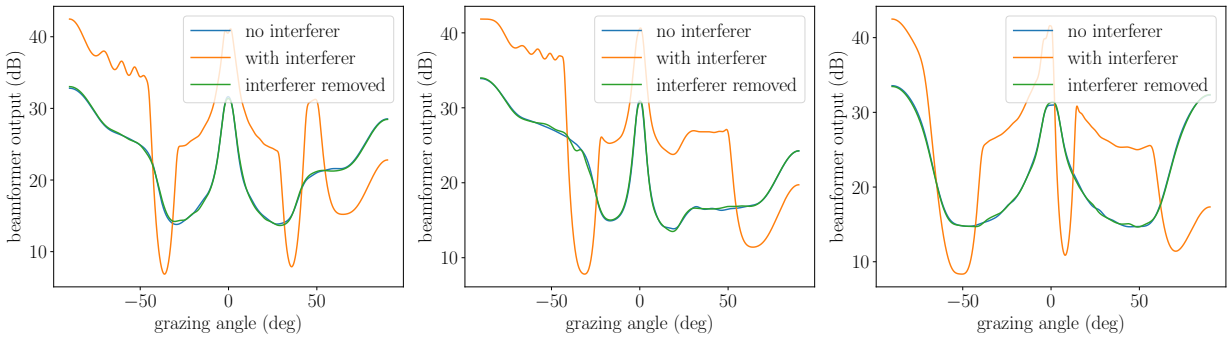

Fig. 3. Estimated vertical directionality curves under absence or presence of rank-2 interference. (a) Type 5 estimates. (b) Type 11 estimates. (c) Type 1 estimates. All recovered curves have a relative error near or below 1%.

We use $L = 1,000$ snapshots to reduce the impact of covariance estimation. Compared with the hypothesis testing results above, the figure demonstrates that low-rank interference of this strength makes estimation completely infeasible, resulting in estimates that differ dramatically from the interference-free setting. To evaluate the curves quantitatively, we compute the relative error compared to using K_θ as defined by Eq. 1 directly, i.e., without using a sample covariance matrix. In the case of Type 5, the relative errors are 0.43% without interference, 39.91% with interference, and 0.89% after recovery. Similarly, for Type 11, the relative errors are 0.56%, 44.09%, and 1.02%; for Type 1 the errors are 0.53%, 45.80%, and 0.57%. These indicate that our recovery method is able to mitigate the impact of interference almost completely for this setting.

We next consider recordings from the NESBA experiments, comparing data collected from the mud patch and shelf break regions. These experiments were carried out from April-May 2021 and include ambient sound recordings captured by a drifting buoy towing a VLA with 16 hydrophones, 1 m spacing, and a sampling frequency of 10 kHz. Recordings from April 26, 2021 were obtained near the mud patch region, while data from April 30, 2021 was collected near the shelf break. The sea state for these recordings was 3.

Fig. 4 shows the magnitude of two example covariance matrices heavily corrupted by low-rank interference, which destroys the expected Toeplitz structure. In particular, the shelf break example in Fig. 4(b) shows a strong rank-1 interferer resulting in a large magnitude signal on hydrophone 16. Although the cause of this disturbance is unclear, the figure demonstrates an example of low-rank interference appearing in real-world recordings. We next perform hypothesis testing on the NESBA recordings. To do so, we first determine the *null* class to be either the mud patch or the shelf break. For a null class having N_0 recordings and an alternate class with N_1 recordings, we compare all unique $N_0 (N_0 - 1)/2$ pairs of same-class recordings, followed by all $N_0 N_1$ pairs of across-class recordings. Fig. 5 shows the resulting likelihood ratio test statistic when comparing covariances when (a) the null class is the mud patch, and (b) the null class is the shelf break. The

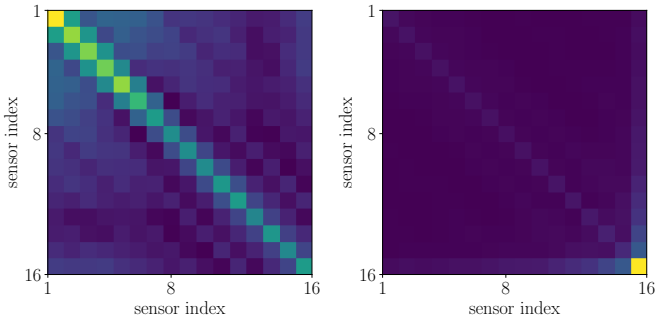

Fig. 4. Magnitude of covariance matrices for example recordings that are heavily corrupted by low-rank interference that destroys Toeplitz structure. (a) Mud patch data, minute 22. (b) Shelf break data, minute 17.

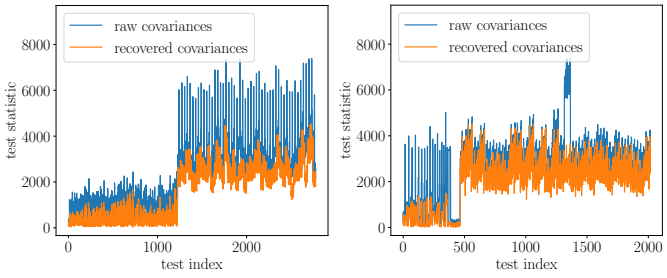

Fig. 5. Test statistic for hypothesis testing on all unique pairs from NESBA recordings. (a) Null class is the mud patch. (b) Null class is the shelf break. Spikes in the test statistic correspond to the covariance shown in Fig. 4(b) and are eliminated by our proposed method.

presence of low-rank interference hampers hypothesis testing, creating many false positives among the shelf break data, seen by the spikes in the first 500 indices of Fig. 5(b). After recovery using our method, hypothesis testing performance is restored to an AUC of 1.0, correctly identifying the corrupted recordings as belonging to the null class.

V. Conclusion

In this paper, we have presented a means for removing low-rank interference from covariance matrices arising from ambient sound collected by a vertical line array. The proposed approach aims to solve a non-convex optimization problem, and we present a method of intelligently initializing this algorithm near the global minimum. The resulting covariance matrices improve both hypothesis testing and vertical directionality estimation, and therefore would likely yield improvements in geoacoustic inversion as well. It would be of theoretical interest to prove whether our initialization method is sufficient to guarantee global convergence under some assumptions (e.g., that the interference is sufficiently non-Toeplitz). A second topic of future study would be to optimize the interferer covariance to maximize the error in vertical directionality estimation in order to provide an understanding of the impact of interference on geoacoustic inversion.

References

[1] D. R. Del Balzo, J. H. Leclere, and M. J. Collins, "Critical angle and seabed scattering issues for active-sonar performance predictions in shallow water," in *High Frequency Acoustics in Shallow Water, Conference Proceedings, 1997*, 1997.

[2] J. Gebbie and M. Siderius, "Optimal environmental estimation with ocean ambient noise," *The Journal of the Acoustical Society of America*, vol. 149, no. 2, pp. 825–834, 2021.

[3] Y.-T. Lin, J. Chaytor, B. J. DeCourcy, G. Gawarkiewicz, J. M. Jech, A. C. Lavery, A. E. Newhall, M. Siderius, W. L. Siegmann, and W. G. Zhang, "Overview of the new england shelf break acoustics (NESBA) experiment," *The Journal of the Acoustical Society of America*, vol. 152, no. 4_Supplement, pp. A26–A26, 2022.

[4] M. Sullivan, J. Gebbie, and J. Lipor, "Adaptive sampling for seabed identification from ambient acoustic noise," in *2023 IEEE 9th International Workshop on Computational Advances in Multi-Sensor Adaptive Processing (CAMSAP)*. IEEE, 2023, pp. 91–95.

[5] Naval Oceanographic Office Acoustics Division, "Database description for bottom sediment type (U)," 2003.

[6] J. Lipor, J. Gebbie, and M. Siderius, "On the limits of distinguishing seabed types via ambient acoustic sound," *The Journal of the Acoustical Society of America*, vol. 154, no. 5, pp. 2892–2903, 2023.

[7] R. R. Wilcox, *Introduction to robust estimation and hypothesis testing*. Academic press, 2011.

[8] P. C. O'Brien, "Robust procedures for testing equality of covariance matrices," *Biometrics*, pp. 819–827, 1992.

[9] J. R. Schott, "Some tests for the equality of covariance matrices," *Journal of statistical planning and inference*, vol. 94, no. 1, pp. 25–36, 2001.

[10] M. S. Srivastava and H. Yanagihara, "Testing the equality of several covariance matrices with fewer observations than the dimension," *Journal of Multivariate Analysis*, vol. 101, no. 6, pp. 1319–1329, 2010.

[11] N. Dörnemann, "Likelihood ratio tests under model misspecification in high dimensions," *Journal of Multivariate Analysis*, vol. 193, p. 105122, 2023.

[12] C. Harrison, "Formulas for ambient noise level and coherence," *The journal of the acoustical society of America*, vol. 99, no. 4, pp. 2055–2066, 1996.

[13] W. K. Stevens, M. Siderius, M. J. Carrier, Y.-T. Lin, and D. Wendeborn, "Ocean ensemble-enabled stochastic acoustic prediction with operational metrics: New england shelf break acoustics signals and noise experiment," *IEEE Journal of Oceanic Engineering*, vol. 48, no. 4, pp. 1187–1214, 2023.

[14] R. A. Johnson and D. W. Wichern, *Applied multivariate statistical analysis*. Pearson, 2007.

[15] T. Anderson, *An Introduction to Multivariate Statistical Analysis*. John Wiley & Sons, 2003.

[16] S. Boyd, N. Parikh, E. Chu, B. Peleato, J. Eckstein *et al.*, "Distributed optimization and statistical learning via the alternating direction method of multipliers," *Foundations and Trends® in Machine learning*, vol. 3, no. 1, pp. 1–122, 2011.

[17] J. P. Boyle and R. L. Dykstra, "A method for finding projections onto the intersection of convex sets in hilbert spaces," in *Advances in Order Restricted Statistical Inference: Proceedings of the Symposium on Order Restricted Statistical Inference held in Iowa City, Iowa, September 11–13, 1985*. Springer, 1986, pp. 28–47.

[18] P. Jain, P. Netrapalli, and S. Sanghavi, "Low-rank matrix completion using alternating minimization," in *Proceedings of the forty-fifth annual ACM symposium on Theory of computing*, 2013, pp. 665–674.

[19] P. Wang, H. Liu, A. M.-C. So, and L. Balzano, "Convergence and recovery guarantees of the k-subspaces method for subspace clustering," in *International Conference on Machine Learning*. PMLR, 2022, pp. 22 884–22 918.

[20] Naval Oceanographic Office Acoustics Division, "Software design description and software test description for the multi-dimensional ambient noise model (MDANM) version 1.01 (U)," 2022.

[21] J. Lipor, J. Gebbie, and M. Siderius, "Understanding and mitigating the impact of passing ships on underwater environmental estimation from ambient sound," *The Journal of the Acoustical Society of America*, vol. 157, no. 2, pp. 811–823, 2025.